Environmental Science Advances

ROYAL SOCIETY OF CHEMISTRY

CRITICAL REVIEW

View Article Online
View Journal | View Issue



Cite this: *Environ. Sci.: Adv.*, 2024, **3**, 1372

# A brief review on flue gas desulfurization gypsum recovery toward calcium carbonate preparation

Wei Xu, *[a] Chunhong Liu,[a] Kaimin Du,[a] Qiangsheng Gao,[a] Zheming Liu[b] and Weijian Wang[b]

The past several years have witnessed great progress in utilization of industrial waste gypsum. Newly developed carbonation technology toward $CaCO_3$ preparation also reveals a significant utilization way to recover high-value products from waste gypsum, whereas there is a shortage of systematic reviews reporting the most recent progress in carbonation of flue gas desulfurization gypsum (FGDG). This review provides a timely and comprehensive summary of major achievements regarding FGDG carbonation and calcium carbonate production to address future investigation directions. We start with a brief introduction of FGDG production and utilization approaches in practical use with their advantages and disadvantages. Then we systematically summarize two types of carbonation, including a direct way and an indirect way. The direct way typically involves three steps: $CO_2$ capture and $CO_3^{2-}$ formation; $CaSO_4 \cdot 2H_2O$ dissolution; $CaCO_3$ crystallization. High purity $CaCO_3$ is prepared and the polymorph of precipitated $CaCO_3$ is affected by many factors, such as the $Ca^{2+}/CO_3^{2-}$ ratio, reaction conditions, impurities, and additives. The indirect way involves gypsum thermal reduction, carbonation, and sulfur recovery. Finally, challenges of current work and perspectives are presented to expedite future industrialization progress and provide a promising research direction for FGDG carbonation.

Received 30th May 2024
Accepted 4th September 2024

DOI: 10.1039/d4va00179f

rsc.li/esadvances



### Environmental significance

The accumulation of a large amount of flue gas desulfurized gypsum (FGDG) not only occupies valuable land resources, but also the harmful substances such as fluorine and heavy metals in FGDG may increase environmental risks. In addition, plants need large quantities of limestone as a desulfurizer. Limestone mainly comes from mining, and the mining process causes significant damage to the regional ecological environment and easily causes personal injury and death accidents. Newly developed technology can transform FGDG into calcium carbonate while capturing $CO_2$ in the flue gas. The development of FGDG carbonation can recover Ca and S resources and contribute to the circular economy.

## 1. Introduction

Flue gas desulfurization gypsum is produced from the capture of $SO_2$ in the flue gas of fossil fuel combustion using Ca-based absorbents.[1–3] Limestone or lime slurry is a widely used Ca-based absorbent.[4] This desulfurization process is as follows:[5,6]

$$SO_2 + H_2O = 2H^+ + SO_3^{2-} \quad (1)$$

$$Ca^{2+} + SO_3^{2-} = CaSO_3 \quad (2)$$

$$1/2O_2 + CaSO_3 = CaSO_4 \quad (3)$$

$$CaSO_4 + 2H_2O = CaSO_4 \cdot 2H_2O \quad (4)$$

Finally, FGDG is produced from the suspension liquid after dewatering and washing. With strict limits on $SO_2$ emissions, every year a huge amount of FGDG is produced.[7,8] According to statistics, FGDG production is about 255 million tons.[9] In China, the yield of FGDG has exceeded 100 million tons since 2017.[5] In India, approximately 20 million tons of FGDG are expected to be generated by the year 2040.[10] Due to the huge amount of production, the treatment of FGDG has become a hot issue in solid waste management in recent years.

The most common application of FGDG is to directly use it in civil infrastructure materials.[11–14] The main component of FGDG is $CaSO_4 \cdot 2H_2O$ with purity more than 90%.[15,16] Thus, it is an ideal material to replace natural gypsum.[17,18] Currently, about 70% of the total FGDG is used as raw material to produce wallboard, gypsum board, whitewashing, cement and concrete in the USA and China.[19–24] However, the supply of FGDG significantly exceeds the demand for building materials, leading to FGDG price dropping. Another application of FGDG in practice is as a resource material in agriculture and soil improvement.[25–28] For example, FGDG can provide S, P, and K

[a]Zhejiang Baima Lake Laboratory Co., Ltd., Hangzhou 310053, P.R. China. E-mail: 21114078@zju.edu.cn
[b]Zhejiang Zheneng Changxing Power Generation Co., Ltd., Huzhou 313100, P.R. China

fertilizers for plant growth and amend saline–alkali soil by exchange of Na.[29,30] Compared to natural gypsum, FGDG has a higher level of heavy metals.[31,32] The content ranges of Hg, Pb, Sb and Zn in FGDG are 0.198–1.33, 1.33–1.84, 4.57–10.9, and 4.26–29 mg $kg^{-1}$, respectively. Hence there is an environmental risk that heavy metals will migrate from FGDG to soil and plants.[33] Nowadays, the consumption of FGDG in agriculture is very limited.

The lack of a utilization way gives rise to serious economy and environmental problems. FGDG treatment is going to be an extra expense for plants. Besides, the accumulation of excessive FGDG will occupy a lot of land, as well as increase the risk of heavy metal leaching. To solve these problems, new approaches have been developed recently.[34] New approaches are aimed at preparing high-value chemicals such as hemihydrate, calcium carbonate, adsorptive materials and composites.[35–42] Among them, preparation of calcium carbonate from FGDG has received great attention. Calcium carbonate is widely used as a filler in polymer composites, paper, plastic, rubber, and pharmaceutical applications.[43–49] Besides, it can also function as a $SO_2$ absorbent in the FGD process. In this way, FGDG is regenerated by the carbonation reaction and then reused in desulfurization, as shown in Fig. 1. Preparation of calcium carbonate from FGDG not only solves the problem of FGDG accumulation and saves the natural resources of $CaCO_3$, but also provides by-products such as sulfur and ammonium sulfate. Furthermore, carbonation with FGDG is conducive to reducing carbon emission, by using $CO_2$ in flue gas as a carbon source. There are mainly two kinds of methods developed for FGDG carbonation, *i.e.* a direct way and an indirect way. The direct way refers to the direct carbonation reaction of FGDG with $CO_2$ and an alkaline reagent at low temperature. The indirect way is first to reduce $CaSO_4$ to CaS or CaO at high temperature and then react it with $CO_2$ to prepare $CaCO_3$.[50,51] However, a summary of recent progress in flue gas desulfurization gypsum recovery toward calcium carbonate preparation is still lacking.

Here we mainly focus on the most advanced development of FGDG application toward $CaCO_3$ preparation. Specifically, we exclusively focus on the carbonation reaction under different conditions and the prepared $CaCO_3$. To deepen comprehension of influence factors, the corresponding mechanism is discussed. We first introduce the direct way to prepare calcium carbonate from FGDG. Then the indirect way with the recovery of sulfur is presented. Finally, a succinct summary of this review and perspectives for future development are provided to lead to an investigation of cost-effective and high-efficiency technology for industrial application.

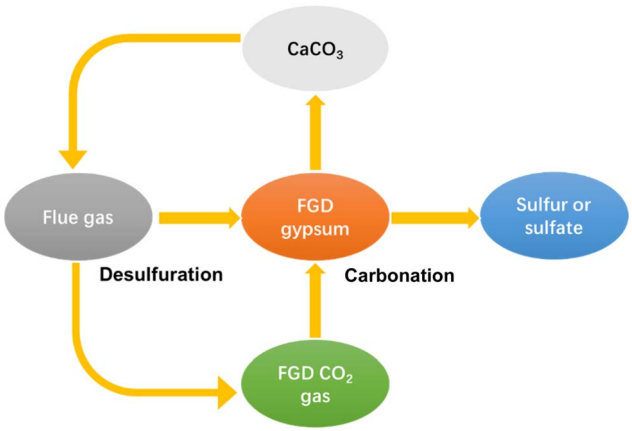


Fig. 1 Schematic diagram of the FGD process with calcium recycling.

## 2. Direct way

### 2.1 Carbonation system and pathway

The direct way is to prepare a calcium carbonate precipitate with waste gypsum at near room temperature. Soluble carbonates such as $Na_2CO_3$ and $NH_4HCO_3$ were used as $CO_3^{2-}$ sources for $CaSO_4$ to $CaCO_3$ conversion in the early research studies.[52,53] Nowadays, with the strong demand for reducing carbon emission, more researchers are devoted to directly convert FGDG to $CaCO_3$ using $CO_2$ gas. The main component of FGDG is $CaSO_4 \cdot 2H_2O$. The carbonation reaction of $CaSO_4 \cdot 2H_2O$ and $CO_2$ proceeds only if the solubility product of $CaSO_4 \cdot 2H_2O$ is larger than that of $CaCO_3$ in the solid–liquid system. At atmospheric $CO_2$ pressure, the solubility products of $CaSO_4 \cdot 2H_2O$ and $CaCO_3$ are affected by pH.[54] According to theoretical calculations, the solubility product of $CaSO_4 \cdot 2H_2O$ is larger than that of $CaCO_3$ at pH > 7.5.[55] This will lead the reaction (5) to proceed rightwards. In contrast, if pH < 7.5, $CaCO_3$ is going to dissolve and the reaction (5) proceeds leftwards.

$$CaSO_4 \cdot 2H_2O + HCO_3^- \leftrightarrow CaCO_3 + H^+ + SO_4^{2-} + 2H_2O \quad (5)$$

Hence, the control of pH conditions is very important for FGDG direct carbonation. In order to achieve high pH conditions, FGDG is mixed with alkaline solution. The alkaline solution is commonly made using sodium hydroxide or ammonia. Accordingly, carbonation systems are named NaOH-FGDG-$CO_2$ and $NH_3$-FGDG-$CO_2$ respectively. As shown in Fig. 2, when using sodium hydroxide as an alkaline reagent, the carbonation processes involve three main steps:[56]

(1) The dissolution of FGDG in alkaline solution to produce $Ca^{2+}$ and $SO_4^{2-}$.

(2) The capture of $CO_2$ gas using alkaline solution and generation of $HCO_3^-$ and $CO_3^{2-}$.

(3) The nucleation of $CaCO_3$ and formation of supersaturation in the solution phase, followed by precipitation.

Similarly, Gong *et al.* put forward multistep carbonation of the $NH_3$–gypsum–$CO_2$ system.[57] It involves $CO_3^{2-}$ formation, $CaSO_4 \cdot 2H_2O$ dissolution, and $CaCO_3$ crystallization. $CO_2$ is absorbed by ammonia to form $NH_2COO^-$, which then hydrolyzes to $NH_3$ and $CO_3^{2-}$. $Ca^{2+}$ in the bulk solution is consumed rapidly with the formation of a $CaCO_3^0$ ion pair. The concentration of the $CaCO_3^0$ ion pair increases and reaches supersaturation. After that, the ion pair concentration decreases gradually, whereas $CaCO_3$ precipitates obviously in the bulk solution. The rates of $CaSO_4 \cdot 2H_2O$ dissolution and $CO_2$ absorption determine the carbonation rate. According to the recent work about FGDG carbonation as listed in Table 1, both

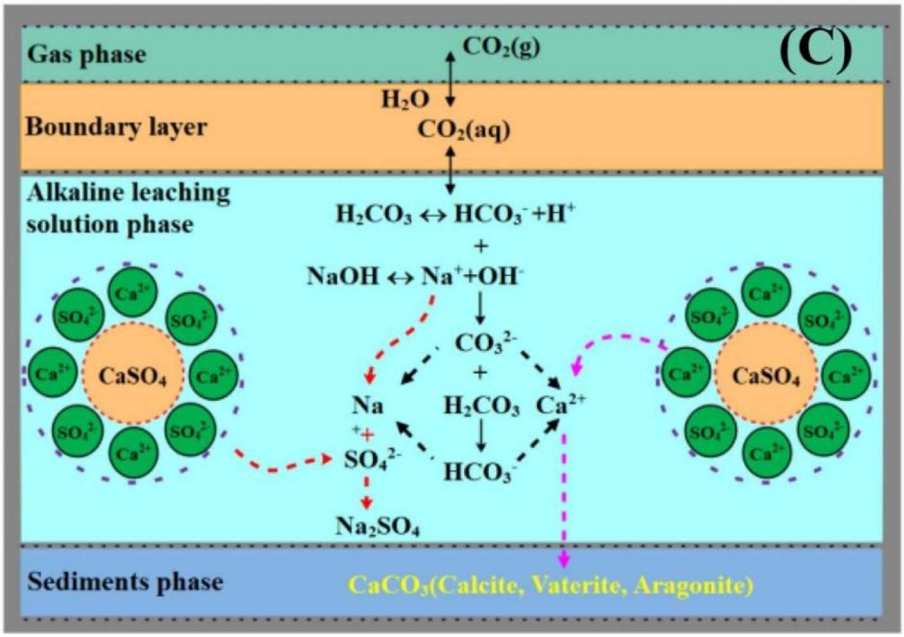


Fig. 2 Schematic diagram of FGDG carbonation processes with sodium hydroxide and $CO_2$ (reprinted with permission from Luo *et al.*[56] Copyright Elsevier 2023).

sodium hydroxide and ammonia are efficient alkaline reagents for FGDG carbonation with more than a 98% conversion ratio achieved. The alkali concentration will affect the conversion ratio. As the NaOH concentration increased from 0.5 mol $L^{-1}$ to 3 mol $L^{-1}$, the conversion ratio increased from 96.4% to 99.94%.[56] Compared to ammonia, sodium hydroxide is more environment-friendly, because it can avoid ammonium volatilization from ammonia.[67] In addition, sodium hydroxide can shorten conversion time of FGDG. However, the by-product of the NaOH-FGDG-$CO_2$ carbonation system is sodium sulfate, and its economic value is relatively low. In comparison, the ammonium sulfate by-product from the $NH_3$-FGDG-$CO_2$ system is a high-value chemical. Besides sodium hydroxide and ammonia, researchers developed FGDG carbonation methods

Table 1 List of published work about FGDG carbonation

| Works | Alkaline reagent | Condition | Solid-to-solution ratio | $CO_2$ gas | Conversion rate | $CaCO_3$ crystal |
|---|---|---|---|---|---|---|
| Luo *et al.*[56] | 3 mol per L NaOH | Stirring | 1 : 8 | 0.0 MPa $CO_2$ | 99.94% | Calcite |
| Luo *et al.*[56] | 3 mol per L NaOH | Stirring | 1 : 8 | 0.2 MPa $CO_2$ | 99.95% | Aragonite |
| Wang *et al.*[58] | 25 wt% ammonia solution | Stirring + ultrasound | — | 99.99% $CO_2$ | 98% | Vaterite |
| Wang *et al.*[59] | 25 wt% ammonia solution | Stirring for 1 h | 10% | 99.99% $CO_2$ | — | 60% vaterite and 40% calcite |
| Tan *et al.*[60] | Aqueous ammonia | — | molar ratio of $NH_3$ to $CaSO_4$ = 2.0 | 99.99% $CO_2$ | 90% at 40 °C, close to 100% at 80 °C | — |
| Lee *et al.*[61] | 25 wt% ammonia solution | Stirring | 15% | 15 wt% $CO_2$, 85 wt% $N_2$ | 96% | Calcite (40–90%) |
| Altiner *et al.*[62] | NaOH or $NH_4OH$ | Stirring | 1 : 13, 1 : 9, and 1 : 7 | 99.99% $CO_2$ | — | Calcite in NaOH and calcite and vaterite in $NH_4OH$ |
| Ding *et al.*[63] | 3 mol per L ammonia solution | Stirring | 20% | 75% $N_2$, 15% $O_2$, 10% $CO_2$ | 90% | Mainly calcite with some vaterite |
| Lee *et al.*[64] | $NH_4OH$, 25 wt% | Stirring | 15–50% | 15% $CO_2$ and 85% $N_2$ | 95% | vaterite and calcite |
| Song *et al.*[51] | Ammonia + ethanol | Stirring | 20% | 99.9% $CO_2$ | — | Calcite and vaterite |
| Liu *et al.*[65] | Glycine + ammonia | Stirring for 1 h | — | Pure $CO_2$ | 97% purity | Vaterite |
| Wang *et al.*[66] | 1.0 mol per L amine | Stirring | 6.8% | 40 vol% $CO_2$ in $N_2$ | 59.8–96.4% | Vaterite (DAP), calcite (PZ) |

by using amine as the alkaline reagent.[66,68,69] Wang *et al.* tested several kinds of amine for FGDG carbonation, including monoethanolamine (MEA), diethanolamine (DEA), triethanolamine (TEA), 1,3-diaminopropane (DAP), piperazine (PZ), 3-amino-1-propanol (MPA), and *N*,*N*-dimethylethanolamine (DEEA).[66] Amines can enhance the absorption of $CO_2$ as well as promote gypsum dissolution by binding amino groups with $Ca^{2+}$. The purity of $CaCO_3$ reached 93.8% when using DAP as the alkaline reagent, which was comparable to 94.4% purity when using the NaOH alkaline reagent. Interestingly, after the carbonation process, the reagent solution was successfully treated by bipolar membrane electrodialysis for amine regeneration and recovery of $H_2SO_4$. This could largely reduce the cost of alkaline consumption.

### 2.2 Mineralization principle and modeling

In an alkaline medium, the driving force of $CO_2$ mineralization of desulfurized gypsum is due to the difference in solubility products between $CaCO_3$ and $CaSO_4 \cdot 2H_2O$ in water. As the solubility product of $CaCO_3$ ($K_{sp} = 4.8 \times 10^{-9}$, 298 K) is much smaller than that of $CaSO_4 \cdot 2H_2O$ ($K_{sp} = 2.6 \times 10^{-5}$, 298 K), the driving force of the reaction is large, and the theoretical conversion rate can reach more than 99%. Several studies have been conducted on modeling the $CO_2$ adoption, ammonium bicarbonate hydrolysis and $CaCO_3$ formation process. Tan *et al.* studied the process parameters of direct wet mineralization of $CO_2$ with desulfurized gypsum and established a reaction model of direct wet mineralization of $CO_2$ with desulfurized gypsum in an ammonia medium system.[60] There is a competition between the $CO_2$ absorption reaction and $NH_2COO^-$ hydrolysis reaction, in which the $CO_2$ absorption reaction dominates over the latter. The $HCO_3^-$ (or $CO_3^{2-}$) from $NH_2COO^-$ hydrolysis is consumed fast to form calcium carbonate, which would enable the $HCO_3^-$ (or $CO_3^{2-}$) concentration to vary little. Liu *et al.* investigated $CaCO_3$ crystal nucleation and growth processes in the gas ($CO_2$)–liquid ($NH_3 \cdot H_2O$)–solid ($CaSO_4$) three-phase system.[70] The research revealed that temperature affected $CaCO_3$ crystal growth more than the nucleation process. They established a model to predict the $CaCO_3$ particle size. Gong *et al.* studied modeling of multistep $Ca^{2+}$ transfer in $CaSO_4$ mineralization using a gypsum disk.[57] The $CaCO_3^0$ ion pair was the intermediate product in $CaCO_3$ induction and nucleation periods. The ion pair determined nucleation and formation of supersaturation. The modeling revealed that $NH_2COO^-$ hydrolysis was the rate-limiting step in induction and nucleation periods, and the dissolution of $CaSO_4 \cdot 2H_2O$ became dominant in the growth period. An increase in the $CO_2$ flow rate can improve $NH_2COO^-$ hydrolysis, leading to more nuclei and high supersaturation. The impeller speed can affect the dissolution rate in the growth period, but it had no remarkable effect on the concentrations of components in induction and nucleation periods.

### 2.3 $CaCO_3$ crystal and utilization

Calcium carbonate is an important raw material in many industrial processes, such as plastics, rubber, tires, paper, building materials, coatings, food, medicine and feed. Certainly, calcium carbonate from FGDG mineralization can be directly functioned as a desulphurization sorbent without impurity separation, because a desulphurization sorbent does not require highly purified $CaCO_3$.[71] Considering the large amount of FGDG, it is a promising way to consume the $CaCO_3$ products. Besides, it can avoid long distance transportation. It's worth noting that calcium carbonate has three polymorphs, namely, calcite, aragonite, and vaterite,[72,73] as shown in Fig. 3. The crystal structure of $CaCO_3$ for FGDG carbonation has received a lot of attention because it determines specific purposes. Because vaterite $CaCO_3$ has good smoothness, fluidity, dispersion and wear resistance, it is widely used in the fields of rubber, paint, ink, medicine, toothpaste and cosmetics.[74]

It can be concluded from Table 1 that vaterite will be produced from FGDG mineralization when using ammonia. The possible principle might be as follows:[58] In the first stage,

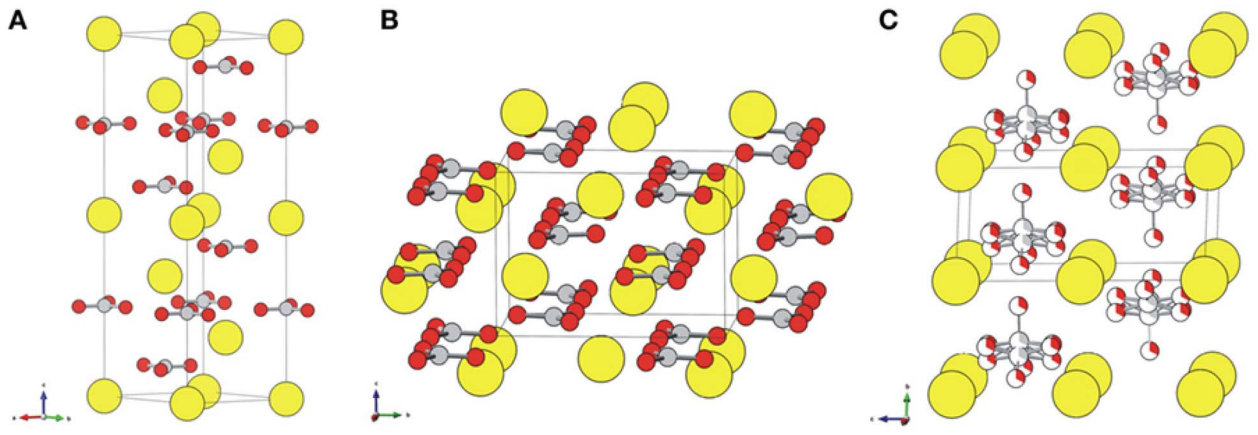


Fig. 3 Crystal structures of (A) calcite, (B) aragonite, and (C) vaterite. Ca atoms are displayed as large yellow balls, and carbonate groups are illustrated with gray (carbon) and red (oxygen) balls. Vaterite is depicted with a hexagonal $P6_3/mmc$ structure that accounts for a partial occupancy of one-third of the carbonate groups. (Reprinted with permission from Chang *et al.*[72] Copyright American Chemical Society 2017.).

the initial $Ca^{2+}$ concentration in the system is low (the solubility of $CaSO_4 \cdot 2H_2O$ is 2 g $L^{-1}$@20 °C, so the initial $Ca^{2+}$ concentration in the solution is about 0.01 M). In the ammonia medium, when $CO_2$ is introduced into the reaction system, $CO_2$ and ammonia will react quickly to produce a large amount of $CO_3^{2-}$; at this time, a very low $Ca^{2+}/CO_3^{2-}$ ratio is conducive to the formation of vaterite.[75] In the second stage, the mixture of $(NH_4)_2CO_3$ and $NH_4HCO_3$ is the main substance.[76] In addition, the concentration of $SO_4^{2-}$ gradually increases with the extension of reaction time, and a higher concentration of $SO_4^{2-}$ can stabilize vaterite in aqueous solution.[77] Therefore, the synergistic effect of low $Ca^{2+}/CO_3^{2-}$ with a higher concentration of $SO_4^{2-}$ may be a key factor in the formation of vaterite in the second stage. In the third stage, the reaction of $HCO_3^-$ with $Ca^{2+}$ to produce vaterite may be due to the high concentration of $SO_4^{2-}$, because a high concentration of $SO_4^{2-}$ can stabilize vaterite in aqueous solution and inhibit its conversion to calcite. Therefore, the combined effect of the above factors promotes the formation of vaterite in the process of FGDG mineralization in the ammonia medium system.

### 2.4 Effect of factors on the $CaCO_3$ polymorph

Much effort has been made to control the polymorph of calcium carbonate from carbonation. The polymorph of $CaCO_3$ is affected by many factors, such as the $Ca^{2+}/CO_3^{2-}$ ratio, reaction conditions, impurities, and additives. The $Ca^{2+}/CO_3^{2-}$ ratio is a key factor related to $CaCO_3$ crystallization growth.[78,79] A high ratio of $Ca^{2+}/CO_3^{2-}$ favors the formation of the calcite.[75] Experiments demonstrated that NaOH solution has a better $Ca^{2+}$ extraction effect than $NH_3 \cdot H_2O$ solution, resulting in a higher $Ca^{2+}/CO_3^{2-}$ ratio in NaOH solution.[80] Thus, it has been found that $CaCO_3$ tends to be pure calcite in the NaOH system, whereas vaterite was achieved in the $NH_3 \cdot H_2O$ system.[81] Another way to reduce the $Ca^{2+}/CO_3^{2-}$ ratio is using high $CO_2$ pressure. Experiments demonstrated that calcite is generated by carbonation with NaOH and atmospheric $CO_2$, while aragonite is generated at $CO_2$ pressure 0.2 MPa.[56] As $CO_2$ pressure increases, $CaCO_3$ particle size becomes larger and purity is 0.7% lower.

Using additives is an effective way to control the $CaCO_3$ polymorph. Liu *et al.* added glycine in the $NH_3$-FGDG-$CO_2$ system.[65] As a result, calcite content in $CaCO_3$ reduced and vaterite content increased. When no glycine is added, around 40% is calcite and 60% is vaterite. When glycine concentration is 20 wt%, vaterite purity reached 97%. They attributed it to the formation of a $Ca(NH_2CH_2COO)_2$ intermediate *via* reactions (6) and (7), which reduced the concentration of $Ca^{2+}$ in bulk solution and provided a lower local $Ca^{2+}/CO_3^{2-}$ ratio. Song *et al.* introduced ethanol into the $NH_3$-FGDG-$CO_2$ system during the induction period.[51] Ethanol might block the surface and inhibit the perfect growth of calcite, by binding more strongly at the calcite surface than with water. Under stoichiometric ammonia conditions, the addition of ethanol gave rise to polymorph change from calcite to vaterite. Under excess-ammonia conditions, peanut-like aragonite crystals with dandelion-like heads were formed when 30 and 50 vol% ethanol were used. However, with ethanol more than 70 vol%, the reaction products were not $CaCO_3$, but were rather compounds composed of $(NH_4)_2SO_4$ and $(NH_4)_2Ca(SO_4)_2 \cdot H_2O$. Polyacrylic acid is proved to enhance gypsum dissolution.[82] With the addition of 2.7 g per L polyacrylic acid in the $NH_3$-FGDG-$CO_2$ system, the amount of dissolved $Ca^{2+}$ increased to 60% of the gypsum. The prepared $CaCO_3$ was amorphous, which could completely crystallize to calcite after exposure to air for 2.5 hours.

$$NH_2CH_2COOH + NH_4OH \rightarrow NH_2CH_2COONH_4 + H_2O \quad (6)$$

$$2NH_2CH_2COONH_4 + CaSO_4 \cdot 2H_2O \rightarrow Ca(NH_2CH_2COO)_2 + (NH_4)_2SO_4 + 2H_2O \quad (7)$$

In general, impurity elements such as Si, Mg, Al, Fe, F and K exist in FGDG,[83] and it's worth noting the influence of impurities. $CaCO_3$ generated from pure $CaSO_4 \cdot 2H_2O$ with $NH_3$–$CO_2$ is 100% vaterite, while from FGDG-$NH_3$-$CO_2$ it is a mixture of vaterite and calcite.[59] According to the XRD results in Fig. 4,[59] dolomite ($CaMg(CO_3)_2$) in $CaSO_4 \cdot 2H_2O$ will lead to the formation of calcite using $NH_3$–$CO_2$. The dolomite particles have a negative charge in the process of carbonation of $CaSO_4 \cdot 2H_2O$, which preferentially adsorb $Ca^{2+}$ through the electrostatic attraction force leading to a higher local ratio of $Ca^{2+}/CO_3^{2-}$. It is reported that $CaSO_4 \cdot 2H_2O$ carbonation at a high ratio of $Ca^{2+}/CO_3^{2-}$ tends to form calcite.[84,85] This may be the reason why different polymorphs are observed. High content of $Mg^{2+}$ or MgO can stabilizing the amorphous $CaCO_3$ produced from precipitate crystallization.[86–88] The presence of F, Fe, and Mg accelerates the conversion rate of calcium carbonate from thermodynamically unstable vaterite to thermodynamically stable calcite.[89,90] The effect of F is more obvious, in all samples with F, and only calcite and no vaterite are present. In the reaction of FGDG carbonation with ammonium carbonate,

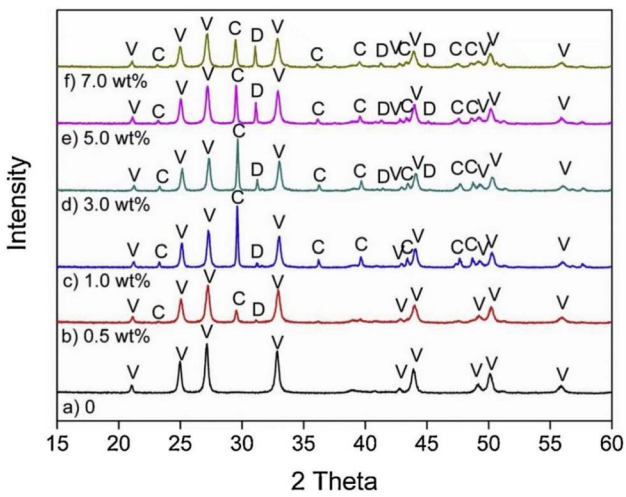


Fig. 4 XRD pattern of $CaCO_3$ obtained in the presence of varying amounts of dolomite particles: (a) $CaCO_3$ sample prepared in the absence of dolomite; (b–f) $CaCO_3$ prepared with 0.5 wt%, 1.0 wt%, 3.0 wt%, 5.0 wt% and 7.0 wt% dolomite particles, respectively. Abbreviations: V, vaterite; C, calcite; D, dolomite. (Reprinted with permission from Wang *et al.*[59] Copyright Elsevier 2019.).

$CO_3^{2-}$ in ammonium carbonate replaces $SO_4^{2-}$ in gypsum to form $CaCO_3$. Therefore, the greater concentration of $CO_3^{2-}$ ions in the solution will be conducive to the reaction. F, Fe and Mg impurities will affect the progress of ammonium carbonate hydrolysis. The hydrolysis of $F^-$ produces $OH^-$, leading to the increase of $CO_3^{2-}$ ions, and the conversion rate is increased. The hydrolysis of $Mg^{2+}$ and $Fe^{3+}$ produces H, which reduces the concentration of $CO_3^{2-}$. $Fe(OH)_3$ and $Mg(OH)_2$ generated from hydrolysis will cover the surface of FGDG with precipitation and reduce the reaction rate and conversion rate. The higher the concentration of $Mg^{2+}$ and $Fe^{3+}$, the more serious the hydrolysis and deposition, and the more the conversion rate is reduced.[91]

Reaction conditions such as temperature, $CO_2$ flow rate, solvent ratio, alkaline concentration and stirring rate are important factors. Temperature has a great influence on $CaCO_3$ polymorphs according to the work by Lee *et al.*[61] At 20 °C and 40 °C, the carbonation product is a mixture of spherical vaterite and calcite with poorly developed edges. At 60 °C, most vaterite will transform into calcite. At 80 °C, needle-flower-like aragonite is newly formed. The use of ultrasound can help control the crystallization process and the formation of $CaCO_3$ polymorphs due to sonocrystallization.[92,93] Application of ultrasound technology in FGDG carbanion can achieve high conversion efficiency and pure vaterite in the ammonia system.[58,94] The $CaSO_4 \cdot 2H_2O$ conversion efficiency is about 60% at 25% ultrasonic amplitude (20 kHz, 650 W), while both conversion efficiencies at 50% and 75% ultrasonic amplitudes were around 98%. The stirring speed has a relatively minor effect on the formation of $CaCO_3$ polymorphs. It mainly affects the particle size and morphologies. Increasing stirring speed can reduce $CaCO_3$ particle size. The particle size at 450 rpm and 675 rpm is 23.45 μm and 18.38 μm, respectively.[56]

### 2.5 FGDG leaching and mineralization technology

As the low solubility of FGDG inhibited the carbonation reaction, researchers developed new mineralization technology with leaching. First, $Ca^{2+}$ is leached from FGDG using a leaching agent. Secondly, the leachate and solid residue are separated. Finally, the $Ca^{2+}$ in the leachate is carbonated to produce $CaCO_3$. By leaching technology, the impurities in FGDG are removed, and thus high purity $CaCO_3$ can be obtained. Several leaching agents have been developed, including inorganic salts and organic leaching agents.

NaCl, $NH_4Cl$ and $CH_3COONH_4$ were inorganic salt based leaching agents. Chen *et al.* explored the mineral mineralization process of phosphogypsum under the action of NaCl and $NH_4OH$.[95] The dissolution efficiency of phosphogypsum under the optimal conditions was 49.42%. One ton of phosphogypsum can chelate 115 kg of $CO_2$ during mineralization and produce 262 kg of $CaCO_3$. In the whole preparation process, NaCl was recycled 4 times, and the corresponding reaction efficiency was above 60%. Ding *et al.* experimentally and theoretically studied the mineral mineralization of phosphogypsum with ammonium acetate.[96] Under the optimal conditions, the dissolution rate of calcium is 98.1% and the mineralization efficiency is 98.32%. The structure of carbonated products was controlled by adjusting the reaction temperature and the amount of ammonia. The phosphogypsum leached with $NH_4Cl$ showed that the optimum dissolved amount of $CaSO_4 \cdot 2H_2O$ was 18.7 g $L^{-1}$ and the carbonation rate was 98.22%.[97]

Organic leaching agents contain carboxyl (–COOH) and amino ($-NH_2$) groups in their molecular structures that can form a soluble chelate with $Ca^{2+}$. Using sodium gluconate as a phase transfer agent, Yang *et al.* synthesized calcium carbonate using phosphogypsum as a raw material at room temperature and atmospheric pressure through a simple and effective "phase transfer – precipitation" route.[98] The results showed that the presence of sodium gluconate inhibited the nucleation and growth of calcite and promoted the formation of vaterite. Gong *et al.* used aspartic acid as the leaching agent, and the results showed the amount of dissolved $CaSO_4 \cdot 2H_2O$ and the total carbonation efficiency during cycling were determined to be 16.3 ± 0.4 g $L^{-1}$ and 46.5 ± 1.9%, respectively.[99]

## 3. Indirect way

### 3.1 Thermal reduction of $CaSO_4$

The indirect way for calcium carbonate preparation from FGDG is quite different from the direct way. Firstly, $CaSO_4$ in gypsum is converted to CaS *via* thermal reduction. Secondly, calcium carbonate is produced *via* CaS carbonation. In the thermal reduction reaction, carbon, carbon monoxide gas or hydrogen gas is used as a reductant and mixed with gypsum at high temperature.[100–102] Typically, carbon is more accessible and thus it has been widely used. The thermal reduction process using carbon as a reductant is present in reaction (8).

$$CaSO_4 \cdot 2H_2O + 2C \rightarrow CaS + 2CO_2 + 2H_2O \quad (8)$$

The reduction reaction is an endothermic reaction. Enthalpy ($\Delta H°$), entropy ($\Delta S°$), and Gibbs-free energy ($\Delta G°$) decrease over the temperature and the proportionality constant ($k$) increases, as shown in Table 2 (data from Tewo *et al.*[103]).

Tewo *et al.* used the Pyrosim Mintek model to predict that $CaSO_4$ to CaS conversion could be increased from 26.8 to 85.0% when the temperature was raised from 500 to 1100 °C.[103] The appropriate temperature range is 700−900 °C for a high conversion ratio.[104] If the temperature exceeds 1000 °C, self-

Table 2 The effect of temperature on $\Delta H°$, $\Delta S°$, $\Delta G°$, and $k$ (data are reproduced with permission from Tewo *et al.*[103] Copyright Elsevier 2019)

| $T$ (°C) | $\Delta H°$ (kJ mol$^{-1}$) | $\Delta S°$ (kJ mol$^{-1}$) | $\Delta G°$ (kJ mol$^{-1}$) | $k$ |
|---|---|---|---|---|
| 25 | 171.0 | 367.0 | 61.5 | $1.7 \times 10^{-11}$ |
| 156 | 172.0 | 367.0 | 13.5 | $2.3 \times 10^{-2}$ |
| 286 | 170.1 | 365.6 | −34.3 | $1.6 \times 10^{3}$ |
| 417 | 167.3 | 361.2 | −81.9 | $1.6 \times 10^{6}$ |
| 547 | 162.9 | 355.4 | −128.7 | $1.6 \times 10^{8}$ |
| 678 | 157.0 | 348.8 | −174.7 | $3.9 \times 10^{9}$ |
| 939 | 141.1 | 334.1 | −263.8 | $2.4 \times 10^{11}$ |
| 1069 | 131.0 | 326.2 | −307.0 | $8.8 \times 10^{11}$ |
| 1200 | 119.7 | 318.1 | −349.0 | $2.4 \times 10^{12}$ |

decomposition reactions and re-reactions probably occur according to reactions (9)–(13). Tan *et al.* conducted thermal reduction experiments with a 2 : 1 weight ratio of FGDG to carbon powder, and gypsum was completely decomposed into calcium sulfide by calcining at 900 °C for 30 min.[105] However, only the oldhamite phase has been observed after in the temperature range of 900 to 1100 °C. Liu *et al.* achieved a FGDG conversion ratio of 97.89% and CaS purity of 90.42% with 30% carbon content after thermal reduction at 900 °C for 2 hours.[104] They indicated that thermal reduction was completed *via* step-by-step reactions, and $SO_4^{2-}$ was transformed into $SO_3^{2-}$–$S_2^{2-}$–$S^{2-}$. Confirmed by a scanning electron micrograph, a hollow structure was formed gradually from the outside to the inside. Phosphogypsum is also a major source of industrial waste gypsum. Laasri *et al.* tested thermal reduction of phosphogypsum by CO gas.[106] At 600 °C, calcium sulfide (CaS) was mainly formed with high CO partial pressure (>50%), and calcium oxide (CaO) was mainly formed with lower CO partial pressure (<20%). At 1000 °C and above, $CaSO_4$ was completely converted to CaS, CaO, and minor co-products due to the presence of impurities in phosphogypsum. One should note that other products were also found after thermal reduction apart from CaS and CaO, such as $Ca_2Fe_2O_5$ and $Ca_2Al(AlSiO_7)$.[107–109] The reason is that $CaSO_4$ will react with the impurities (Al, Fe, Si *etc.*) in gypsum at high temperature.

$$CaSO_4 \rightarrow CaO + SO_2 + 0.5O_2 \quad (9)$$

$$CaS + 3CaSO_4 \rightarrow 4CaO + 4SO_2 \quad (10)$$

$$3CaS + CaSO_4 \rightarrow 4CaO + 2S_2 \quad (11)$$

$$CaS + 2O_2 \rightarrow CaSO_4 \quad (12)$$

$$CaS + 1.5O_2 \rightarrow CaO + SO_2 \quad (13)$$

The carbon to gypsum ratio is a vital factor. Insufficient carbon content will lead to a low conversion efficiency. However, too much carbon will result in carbon waste and low CaS purity. It is reported that there is an increasing trend in conversion efficiency from 57.4 to 83.8% when the carbon ratio is increased from 1 : 1 to 4 : 1.[103] Liu *et al.* investigated the relationship between carbon content and conversion.[104] At 10% carbon content, conversion efficiency was about 41% with 25% CaS purity. The conversion efficiency increased to above 97% and the CaS purity was about 90% at 30% carbon content. Further increasing the carbon content had a slight influence on conversion efficiency, but the CaS purity reduced less than 80% due to carbon residues. Motaung *et al.* made pelletized gypsum from acid mine drainage (AMD) neutralization by adding starch or cellulose as a binder into a mixture of gypsum and coal.[110] The CaS yield of pelletized gypsum thermo-reduction was improved from 60% without starch or cellulose to 71% or 67% with 8% starch or cellulose, respectively. The CaS yield could further reach above 90% with gypsum and starch at a ratio of 1 : 2.9 at 1050 °C for 20 min.

### 3.2 CaS carbonation and sulfur recovery

The produced CaS can react with $H_2O$ and $CO_2$ for carbonation *via* reaction (14). However, the produced $CaCO_3$ is low-grade (*i.e.* <90 mass%) which comprised a mixture of calcite and vaterite.[102] Carbonation of CaS is difficult and sluggish in aqueous solution, and more than 3 hours are needed for $CaCO_3$ to occur.[105] This is due to CaS being a sparingly soluble salt in water.[111] Accordingly, de Beer developed a new carbonation method by sparging $H_2S$ gas to aqueous CaS suspensions.[50] $H_2S$ reacted with CaS to form water-soluble $Ca(HS)_2$ *via* reaction (15). Thus 91.7% CaS was extracted into the aqueous phase and separated from the impurities in the solid phase. Then $CO_2$ gas is introduced for carbonation by reaction (16). High purity

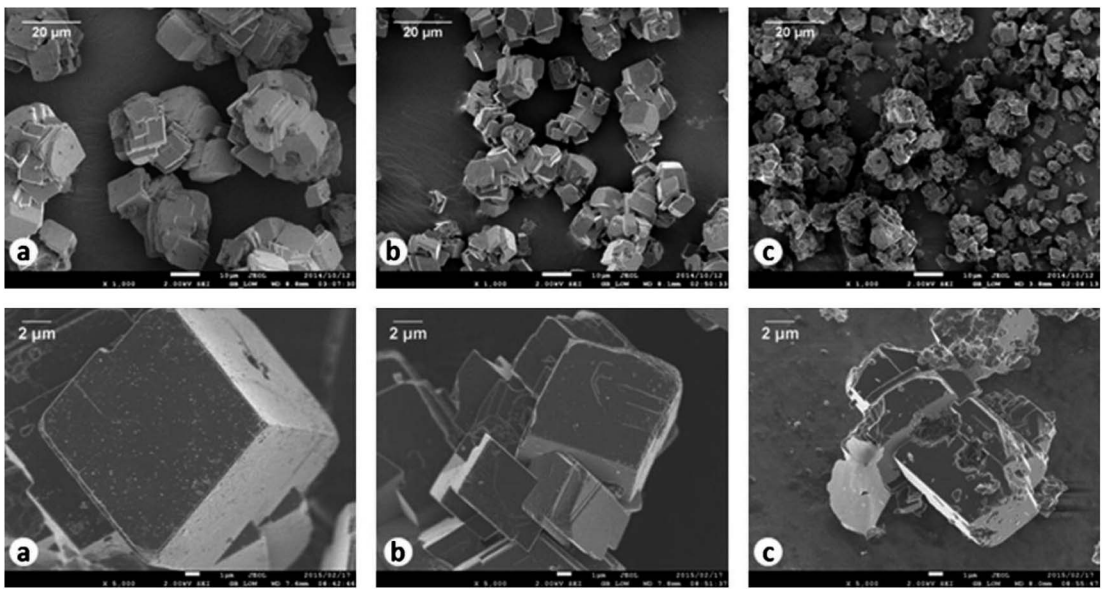


Fig. 5 SEM images (top row 1000× and bottom row 5000× magnification) of high-grade $CaCO_3$ produced at initial $Ca^{2+}$ concentrations of (a) 450 mmol $L^{-1}$, (b) 900 mmol $L^{-1}$ and (c) 1800 mmol $L^{-1}$. (Reprinted with permission from de Beer *et al.*[50] Copyright Elsevier 2015.).

(99.5%) $CaCO_3$ is produced. Rhombohedral structured calcites with different particle sizes were demonstrated after $Ca(HS)_2$ carbonation with different initial $Ca^{2+}$ concentrations, as shown in Fig. 5.

$$CaS + H_2O + CO_2(g) \rightarrow H_2S(g) + CaCO_3 \quad (14)$$

$$CaS + H_2O + H_2S \rightarrow Ca(HS)_2 + H_2O \quad (15)$$

$$Ca(HS)_2 + H_2O + CO_2 \rightarrow CaCO_3 + H_2S \quad (16)$$

The $H_2S$ produced in reactions (14) and (16) can be further oxidized to high-value elemental sulfur.[112,113] High pH (9.0) is required for the dissolution of hydrogen sulfide, and Fe-based chelates are widely used to promote the reaction. The main chemical reaction can be simplified in reaction (17):[114]

$$H_2S + 2Fe^{3+}L^{n-} \rightarrow S^0 + 2Fe^{2+}L^{n-} + 2H^+ \quad (17)$$

where $L^{n-}$ denotes an organic ligand with $n-$ charges and $S^0$ represents a zero-valence sulfur product. Tan *et al.* successfully recovered elemental sulfur with 0.5–3 μm in diameter from FGDG.[105]

# 4. Perspectives

## 4.1 Technical and economic analyses

Although many studies have reported that a high FGDG conversion rate can be achieved, the results are obtained from bench and pilot scale units. There are still many challenges to further development of practical engineering projects. Cost and profit mainly depended on the raw materials (ammonia or sodium hydroxide) and byproducts (ammonium sulfate, sodium sulfate, and elemental sulfur). However, the prices of these chemicals fluctuate wildly, leading to an economic uncertainty. Raw material sources and byproduct utilization deserve further investigation for practical engineering projects. Advanced technologies to produce high quality $CaCO_3$ *via* impurity separation and polymorph control are also beneficial for practical economic viability. Table 3 summarizes the comparison of FGDG carbonation approaches. The challenges that each face in approaching practical application are discussed in detail in this section.

The direct way has many advantages such as convenient operation, low energy cost and high conversion rates, and it is promising for scaling up. FGDG carbonation can be accomplished in a single step, which is very beneficial to reduce equipment investment and post-production operation. The direct way is carried out under mild reaction conditions, with temperature less than 100 °C and pressure less than 0.2 MPa. According to economic analysis, energy cost for 1 ton of FGDG is about 1.4 ton of steam and 150 kW h of electricity, including the crystallization process of the ammonium sulfate by-product.[36] According to the data in Table 1, conversion rates of $CaSO_4$ can reach more than 90%, and some even approach 100%. Developing large reactors on an industrial scale is a technical key point to achieve satisfactory conversion rates on a large scale. It is worth noting that Cl and F are enriched in FGDG from flue gas.[115,116] The issues of equipment corrosion by Cl and F should be taken into consideration in practical use. Another challenge is the value of the sulfate by-product. For the NaOH-FGDG-$CO_2$ approach, $Na_2SO_4$ is produced. For the $NH_3$-FGDG-$CO_2$ approach, $(NH_4)_2SO_4$ is produced. We have conducted a market survey on the price of raw materials in China, and the price of $(NH_4)_2SO_4$ is three to five times that of $Na_2SO_4$. Thus, the $NH_3$-FGDG-$CO_2$ approach is more scalable in economy. However, if a large amount of $(NH_4)_2SO_4$ is produced from FGDG, there would be a risk of price drop. Besides, the ammonia escape is still a common environmental problem.[117–119]

The indirect way is a multistep approach, which is more complicated than the direct way. The FGDG thermal reduction step requires high temperature around 1000 °C, resulting in large energy consumption. The energy input is about 4060 kJ per kg-FGDG for thermal reduction.[120] As for the indirect way, it is meaningful to combine it with other industrial processes which produce plenty of cheap methane, hydrogen, carbon dioxide and petroleum coke by-products.[121–123] Beneficially, the indirect way can avoid the evaporative crystallization process and save energy. In comparison, the conversion rate of the indirect way is lower than that of the direct way. The FGDG to CaS efficiency is usually less than 90%. Efforts should be made to develop optimum reaction conditions as well as efficient reaction devices. One advantage of the indirect way is that it is possible to prepare high purity $CaCO_3$ from CaS. By forming water-soluble $Ca(HS)_2$, water-insoluble impurities are removed, and the $CaCO_3$ purity reaches 99.5%.[50]

## 4.2 Direct way coupled with NaOH regeneration

The direct way has many technical advantages and is promising for practical use. But stakeholders are usually more concerned about economic feasibility. Raw materials and energy consumption are the main operation costs. Raw materials

Table 3 Comparison of the direct way and indirect way

| Approaches | Reaction processes | Technical and economic analyses |
|---|---|---|
| Direct way | NaOH-FGDG-$CO_2$ or $NH_3$-FGDG-$CO_2$ | Advantages of simple processes, high conversion rates and mild reaction condition. Issues of ammonia escape, device corrosion and by-product application |
| Indirect way | 1. Thermal reduction; 2. CaS carbonation; 3. elemental sulfur preparation | Insufficient conversion rate. High purity $CaCO_3$. Suitable for factories with cheap energy sources |

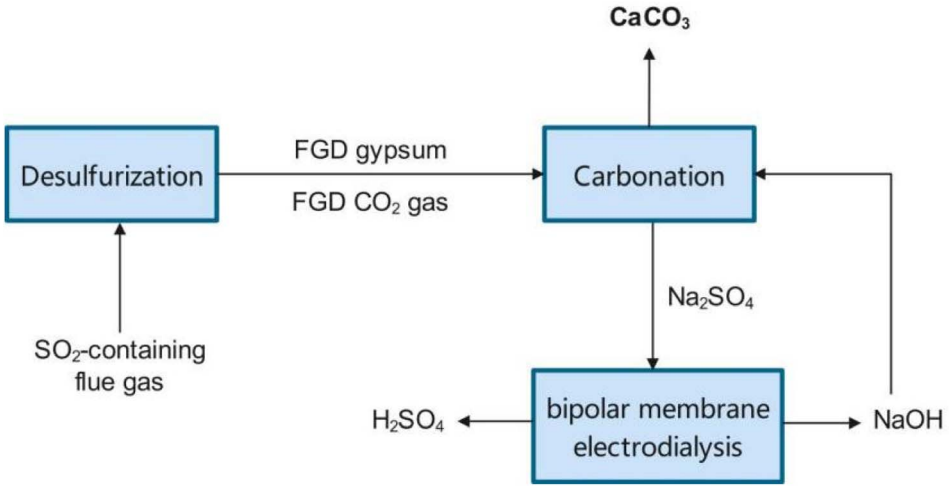


Fig. 6 Schematic diagram of FGDG carbonation coupled with bipolar membrane electrodialysis.

depend on the price of NaOH or $NH_3OH$. Energy is mainly consumed in the crystallization of the $Na_2SO_4$ or $(NH_4)_2SO_4$ by-product. Wang *et al.* proposed a way to apply amine for carbonation and recycle the protonated amine by bipolar membrane electrodialysis (BMED).[66] Inspired by their work, it may be feasible to develop a NaOH–$Na_2SO_4$ circular system by bipolar membrane electrodialysis to reduce the cost of NaOH consumption and avoid energy consumption for crystallization.[124] As shown in Fig. 6, by introducing bipolar membrane electrodialysis into the NaOH-FGDG-$CO_2$ system, the by-product of $Na_2SO_4$ can be split into NaOH and $H_2SO_4$.[125] In this way, the *in situ* regenerated NaOH is reused for FGDG carbonation, instead of raw material procurement. Operation cost comparisons are shown in Table 4. The data of energy consumption for direct FGDG mineralization without BMED were obtained from a pilot plant at a scale of 3 ton per day located in Zhejiang Province, China. For 1000 kg of FGDG, reaction heating consumes about 400 kg of steam and evaporative crystallization consumes about 1000 kg of steam. The quantities of raw materials and products are calculated according to the stoichiometric ratio. When 1000 kg of FGDG was used, 476 kg of $CaCO_3$ and 676 kg of $Na_2SO_4$ were produced with the use of 381 kg of NaOH. Likewise, 629 kg of $(NH_4)_2SO_4$ was obtained when using 334 kg of ammonia. The price of chemicals is the market price in China. The operation costs for NaOH-FGDG-$CO_2$ and $NH_3$-FGDG-$CO_2$ approaches to process 1

Table 4 Operation cost comparisons of the direct way with and without BMED

| | | $NH_3$-FGDG-$CO_2$ | NaOH-FGDG-$CO_2$ | NaOH-FGDG-$CO_2$ with BMED |
|---|---|---|---|---|
| **Materials input** | | | | |
| Ammonia | Input | 334 kg | 0 | 0 |
| | Cost | $175 USD | 0 | 0 |
| NaOH | Input | 0 | 381 kg | 0 |
| | Cost | 0 | $164 USD | 0 |
| **Energy input** | | | | |
| Steam | Input | 1400 kg | 1400 kg | 400 kg |
| | Cost | $59 USD | $59 USD | $17 USD |
| Electricity | Input | 0 | 0 | 1143 kW h |
| | Cost | 0 | 0 | $114 USD |
| **Product output** | | | | |
| $CaCO_3$ | Output | 476 kg | 476 kg | 476 kg |
| | Income | $55 USD | $55 USD | $55 USD |
| $(NH_4)_2SO_4$ | Output | 629 kg | 0 | 0 |
| | Income | $115 USD | 0 | 0 |
| $Na_2SO_4$ | Output | 0 | 676 kg | 0 |
| | Income | 0 | $29 USD | 0 |
| $H_2SO_4$ | Output | 0 | 0 | 460 kg |
| | Income | 0 | 0 | $10 |
| Total cost | | $64 USD | $139 USD | $66 USD |

ton of FGDG are $139 and $64, respectively. The difference is mainly due to the market price variance of $Na_2SO_4$ and $(NH_4)_2SO_4$. Although the $NH_3$-FGDG-$CO_2$ approach demonstrates better cost-effectiveness, the use of ammonia increases environmental risks. Interestingly, by coupling BMED with the NaOH-FGDG-$CO_2$ approach, operation cost is reduced to $67, close to that of $NH_3$-FGDG-$CO_2$. The energy consumption value of BMED is set to 3 kW h per kg-NaOH according to reported data.[118,126] This is mainly due to the saving of raw materials and steam consumed by evaporation crystallization. Considering that raw material prices are wildly affected by the market, BMED is a promising way to obtain sustainable alkaline supply and withstand market risk.

## 5. Conclusion

In this review, we mainly summarize the most recent developments of calcium carbonate recovery from FGDG. There are mainly two kinds of methods developed for FGDG carbonation. *i.e.* the direct way and indirect way. The direct way is gypsum carbonation with $CO_2$ in alkaline solution at near room temperature. The indirect way is thermal reduction of gypsum first and then carbonation of the thermal reduction product.

The direct way typically involves three stages: $CO_2$ capture and $CO_3^{2-}$ formation; $CaSO_4 \cdot 2H_2O$ dissolution; $CaCO_3$ crystallization. NaOH-FGDG-$CO_2$ and $NH_3$-FGDG-$CO_2$ are widely studied carbonation systems. The polymorph of $CaCO_3$ is affected by many factors, such as the $Ca^{2+}/CO_3^{2-}$ ratio, reaction conditions, impurities, and additives.

The indirect way involves gypsum thermal reduction, carbonation, and sulfur recovery. Thermal reduction is preferred to achieve a high conversion ratio at around 900 °C with the addition of carbon as the reductant. The carbonation of CaS is sluggish and produces low purity $CaCO_3$ and $H_2S$ gas by-products. Transformation of CaS into $Ca(HS)_2$ by $H_2S$ before carbonation can purify the $CaCO_3$ product. Finally, high-value elemental sulfur can be recovered from $H_2S$ oxidation.

In comparison, the direct way has advantages of simple processes, a high conversion rate and mild reaction conditions. The indirect way can obtain high purity $CaCO_3$ and is suitable for factories with cheap energy sources. The combination of the direct way and BMED technique has significant advantages. Although there are several approaches developed for FGDG carbonation, pilot and industrial applications are needed to study technical and economic feasibility in the future.

## Data availability

No primary research results, software or code have been included and no new data were generated or analysed as part of this review.

## Author contributions

Wei Xu contributed to conceptualization, writing of the original draft, review & editing. Chunhong Liu contributed to conceptualization, writing – review & editing. Kaimin Du contributed to conceptualization and writing of the original draft. Qiangsheng Gao contributed to writing – review & editing. Zheming Liu contributed to writing – review & editing. Weijian Wang contributed to writing of the original draft.

## Conflicts of interest

There are no conflicts to declare.

## Acknowledgements

This research was supported by the Zhejiang Energy Group Science and Technology Project.

## References

1 T. Cheng, X. C. Zhou, L. J. Yang, Z. Q. Sun and H. Wu, *Energy Fuels*, 2020, **34**, 3836–3842.
2 Z. Xu, D. Hu, R. An, L. Lin, Y. Xiang, L. Han, Y. Yu, L. Ning and J. Wu, *Case Stud. Constr. Mater.*, 2022, **17**, e01549.
3 S. Jian, X. Yang, W. Gao, B. Li, X. Gao, W. Huang, H. Tan and Y. Lei, *Constr. Build. Mater.*, 2021, **301**, 124341.
4 T. Y. Qi, J. Z. Zhang, T. Li, S. L. An, Q. W. Li and L. D. Wang, *Appl. Surf. Sci.*, 2024, **648**, 158981.
5 S. Liu, W. Liu, F. Jiao, W. Qin and C. Yang, *Environ. Pollut.*, 2021, **288**, 117799.
6 S. J. Chen, T. Q. Jiang, H. W. Zhang, K. Kong and L. S. Bie, *Energy Sci. Eng.*, 2020, **8**, 2662–2679.
7 H. S. Guo, Q. P. Wang, W. F. Li, X. Feng, J. L. Yang, J. J. Cao, T. Z. Shen, X. M. Qin, Y. F. Liu, Y. H. Gui and L. M. Zhou, *Constr. Build. Mater.*, 2023, **377**, 130981.
8 M. J. Li, G. D. Huang, B. Wang, Y. Cui, B. B. Chang, Q. Q. Yin, M. Ge, S. W. Zhang, Q. Wang and J. C. Feng, *Polymers*, 2022, **14**, 4761.
9 Aakriti, S. Maiti, N. Jain and J. Malik, *Constr. Build. Mater.*, 2023, **393**, 131918.
10 P. Bakshi, A. Pappu and M. K. Gupta, *J. Mater. Cycles Waste Manage.*, 2022, **24**, 49–62.
11 N. H. Koralegedara, P. X. Pinto, D. D. Dionysiou and S. R. Al-Abed, *J. Environ. Manage.*, 2019, **251**, 109572.
12 J. Y. Hao, G. J. Cheng, T. Hu, B. Guo and X. J. Li, *Constr. Build. Mater.*, 2021, **306**, 124910.
13 C. X. Wu, J. H. He, K. Wang, L. Yang and F. Z. Wang, *Constr. Build. Mater.*, 2023, **387**, 131565.
14 P. Maichin, P. Jitsangiam, T. Nongnuang, K. Boonserm, K. Nusit, S. Pra-ai, T. Binaree and C. Aryupong, *Materials*, 2021, **14**, 1858.
15 P. Córdoba, *Fuel*, 2015, **144**, 274–286.
16 A. Myka, R. Łyszczek, A. Zdunek and P. Rusek, *J. Therm. Anal. Calorim.*, 2022, **147**, 9923–9934.
17 T. Sithole, T. Mashifana, D. Mahlangu and L. Tchadjie, *Buildings*, 2021, **11**, 500.
18 E. Baran, S. Czernik, M. Hynowski, B. Michałowski, M. Piasecki, J. Tomaszewska and J. Michalak, *Sustainability*, 2021, **13**, 4298.

19 J. Li, X. Zhuang, C. Leiva, A. Cornejo, O. Font, X. Querol, N. Moeno, C. Arenas and C. Fernández-Pereira, *Constr. Build. Mater.*, 2015, **95**, 910–921.
20 L. Xu, K. Wu, N. Li, X. Zhou and P. Wang, *J. Cleaner Prod.*, 2017, **161**, 803–811.
21 S. Wansom, P. Chintasongkro and W. Srijampan, *Cem. Concr. Compos.*, 2019, **103**, 134–148.
22 Q. Wu, H. Ma, Q. Chen, Z. Huang, C. Zhang and T. Yang, *Constr. Build. Mater.*, 2019, **214**, 318–325.
23 L. Yang, M. Jing, L. Lu, X. Zhu, P. Zhao, M. Chen, L. Li and J. Liu, *Constr. Build. Mater.*, 2020, **257**, 119519.
24 H. A. Nguyen, C. T. Chen, T. P. Chang and J. Y. Shih, *J. Therm. Anal. Calorim.*, 2023, 13761–13773, DOI: **10.1007/s10973-023-12715-y**.
25 H. Kaur, K. W. J. Williard, J. E. Schoonover and G. Singh, *Water, Air, Soil Pollut.*, 2022, **233**, 72.
26 S. F. Acuña-Guzman and L. D. Norton, *Sustainability*, 2023, **15**, 1977.
27 D. B. Watts, G. B. Runion and H. A. Torbert, *Horticulturae*, 2021, **7**, 199.
28 J. Wang, A. Q. Zhao, F. Ma, J. L. Liu, G. J. Xiao and X. Xu, *Sustainability*, 2023, **15**, 8658.
29 J. Wang and P. Yang, *Renewable Sustainable Energy Rev.*, 2018, **82**, 1969–1978.
30 W. C. Zhang, Y. G. Zhao, S. J. Wang, Y. Li, Y. Q. Zhuo and J. Liu, *Land Degrad. Dev.*, 2021, **32**, 4193–4202.
31 P. Sundha, R. Mukhopadhyay, N. Basak, A. K. Rai, S. Bedwal, S. Patel, S. Kumar, H. Kaur, P. Chandra, P. C. Sharma, S. K. Saxena, S. S. Parihar and R. K. Yadav, *Sci. Rep.*, 2023, **13**, 19787.
32 Z. X. Liu, Y. Hao, J. Zhang, S. M. Wu, Y. Pan, J. Z. Zhou and G. R. Qian, *Fuel*, 2020, **271**, 117515.
33 Y. M. Huang, J. L. Liu, G. Wang, X. Y. Bi, G. Y. Sun, X. Wu, Q. F. Wang and Z. G. Li, *Int. J. Environ. Res. Public Health*, 2022, **19**, 12617.
34 J. Gao, Q. Li and F. L. Liu, *Chin. J. Chem. Eng.*, 2020, **28**, 2221–2226.
35 G. Chen, R. Liu, C. Song and J. Luo, *J. Cryst. Growth*, 2021, **576**, 126360.
36 C.-U. Kang, S.-W. Ji and H. Jo, *Sustainability*, 2022, **14**, 4436.
37 Y. Yan, X. Dong, X. Sun, X. Sun, J. Li, J. Shen, W. Han, X. Liu and L. Wang, *J. Colloid Interface Sci.*, 2014, **429**, 68–76.
38 Y. Liu, Y. Zhang, Y. Guo, P. K. Chu and S. Tu, *Waste Biomass Valorization*, 2017, **8**, 203–207.
39 J. Kang, X. Gou, Y. Hu, W. Sun, R. Liu, Z. Gao and Q. Guan, *Sci. Total Environ.*, 2019, **649**, 344–352.
40 P. Bakshi, A. Pappu and D. K. Bharti, *Mater. Lett.*, 2022, **308**, 131177.
41 D. M. Wang, C. Chen, Y. B. Wang, S. Jiu and Y. X. Chen, *Constr. Build. Mater.*, 2023, **394**, 132280.
42 X. M. Chen, J. M. Gao, Y. Wu, Q. H. Wu and L. Luo, *Materials*, 2022, **15**, 2691.
43 C.-q. Li, C. Liang, Z.-m. Chen, Y.-h. Di, S.-l. Zheng, S. Wei and Z.-m. Sun, *J. Cent. South Univ.*, 2021, **28**, 2589–2611.
44 M. Baláž, E. V. Boldyreva, D. Rybin, S. Pavlović, D. Rodríguez-Padrón, T. Mudrinić and R. Luque, *Front. Bioeng. Biotechnol.*, 2021, **8**, 612567.
45 J. Luo, F. Kong and X. Ma, *Cryst. Growth Des.*, 2016, **16**, 728–736.
46 K. Longkaew, A. Gibaud, W. Tessanan, P. Daniel and P. Phinyocheep, *Polymers*, 2023, **15**, 4287.
47 O. Ersoy and H. Köse, *Polym. Compos.*, 2020, **41**, 3483–3490.
48 Z. L. Liu, W. Y. Liu, L. Y. Ma, M. Mo, Y. F. Huang, W. Q. Lai, M. X. Xu, Y. M. Li, Q. F. Mo, X. J. Bai, C. Chen, Z. M. Huang and Y. H. Zheng, *Polym. Compos.*, 2023, 1494–1507, DOI: **10.1002/pc.27869**.
49 T. Ahmed, H. H. Ya, R. Khan, A. Lubis and S. Mahadzir, *Materials*, 2020, **13**, 3333.
50 M. de Beer, F. J. Doucet, J. P. Maree and L. Liebenberg, *Waste Manage.*, 2015, **46**, 619–627.
51 K. Song, W. Kim, J.-H. Bang, S. Park and C. W. Jeon, *Mater. Des.*, 2015, **83**, 308–313.
52 A. Azdarpour, M. A. Karaei, H. Hamidi, E. Mohammadian, M. Barati and B. Honarvar, *Int. J. Miner. Process.*, 2017, **169**, 27–34.
53 L. Fernández-Díaz, C. M. Pina, J. M. Astilleros and N. Sánchez-Pastor, *Am. Mineral.*, 2009, **94**, 1223–1234.
54 Y. Zarga, H. Ben Boubaker, N. Ghaffour and H. Elfil, *Chem. Eng. Sci.*, 2013, **96**, 33–41.
55 L. Yu, L. M. Daniels, J. J. P. A. Mulders, G. D. Saldi, A. L. Harrison, L. Liu and E. H. Oelkers, *Chem. Geol.*, 2019, **525**, 447–461.
56 X. Luo, C. Wei, X. Li, Z. Deng, M. Li and G. Fan, *Fuel*, 2023, **333**, 126305.
57 Y. Gong, L. Wu, J. Li and J. Zhu, *J. Cryst. Growth*, 2019, **522**, 128–138.
58 B. Wang, Z. Pan, H. Cheng, Y. Guan, Z. Zhang and F. Cheng, *Environ. Chem. Lett.*, 2020, **18**, 1369–1377.
59 B. Wang, Z. Pan, Z. Du, H. Cheng and F. Cheng, *J. Hazard. Mater.*, 2019, **369**, 236–243.
60 W. Tan, Z. Zhang, H. Li, Y. Li and Z. Shen, *Environ. Sci. Pollut. Res.*, 2017, **24**, 8602–8608.
61 M. G. Lee, K. W. Ryu, S. C. Chae and Y. N. Jang, *Environ. Technol.*, 2015, **36**, 106–114.
62 M. Altiner, *Int. J. Coal Prep. Util.*, 2019, **39**, 113–131.
63 W. Ding, H. Yang and J. Ouyang, *RSC Adv.*, 2015, **5**, 67184–67194.
64 M. g. Lee, Y. N. Jang, K. w. Ryu, W. Kim and J.-H. Bang, *Energy*, 2012, **47**, 370–377.
65 X. Liu, B. Wang, Z. Zhang, Z. Pan, H. Cheng and F. Cheng, *Environ. Chem. Lett.*, 2022, **20**, 2261–2269.
66 Y. Wang, X. Zheng, Y. Wang, Q. He, S. Yan and L. Ji, *Chem. Eng. J.*, 2023, **478**, 147335.
67 W. Liu, B. B. Wu, X. X. Bai, S. H. Liu, X. Y. Liu, Y. Hao, W. Z. Liang, S. M. Lin, H. J. Liu, L. N. Luo, S. Zhao, C. Y. Zhu, J. M. Hao and H. Z. Tian, *Environ. Sci. Technol.*, 2020, **54**, 390–399.
68 W. Liu, L. Teng, S. Rohani, Z. Qin, B. Zhao, C. C. Xu, S. Ren, Q. Liu and B. Liang, *Chem. Eng. J.*, 2021, **416**, 129093.
69 Z. Yan, Y. Wang, H. Yue, C. Liu, S. Zhong, K. Ma, W. Liao, S. Tang and B. Liang, *ACS Sustain. Chem. Eng.*, 2021, **9**, 8238–8248.
70 H. Liu, P. Lan, S. Lu and S. Wu, *J. Cryst. Growth*, 2018, **492**, 114–121.

71 M. Altiner, S. Top, B. Kaymakoğlu, İ. Y. Seçkin and H. Vapur, *J. $CO_2$ Util.*, 2019, **29**, 117–125.
72 R. Chang, D. Choi, M. H. Kim and Y. Park, *ACS Sustain. Chem. Eng.*, 2017, **5**, 1659–1667.
73 A. Katsman, I. Polishchuk and B. Pokroy, *Faraday Discuss.*, 2022, **235**, 433–445.
74 D. B. Trushina, T. V. Bukreeva, M. V. Kovalchuk and M. N. Antipina, *Mater. Sci. Eng., C*, 2014, **45**, 644–658.
75 Y. S. Han, G. Hadiko, M. Fuji and M. Takahashi, *J. Eur. Ceram. Soc.*, 2006, **26**, 843–847.
76 H. Chen, B. Dou, Y. Song, Y. Xu, X. Wang, Y. Zhang, X. Du, C. Wang, X. Zhang and C. Tan, *Int. J. Greenhouse Gas Control*, 2012, **6**, 171–178.
77 I. Cuesta Mayorga, J. M. Astilleros and L. Fernández-Díaz, *Minerals*, 2019, **9**, 178.
78 S. Seepma, S. E. Ruiz-Hernandez, G. Nehrke, K. Soetaert, A. P. Philipse, B. W. M. Kuipers and M. Wolthers, *Cryst. Growth Des.*, 2021, **21**, 1576–1590.
79 M. Wolthers, G. Nehrke, J. P. Gustafsson and P. Van Cappellen, *Geochim. Cosmochim. Acta*, 2012, **77**, 121–134.
80 S. M. Pérez-Moreno, M. J. Gázquez and J. P. Bolívar, *Chem. Eng. J.*, 2015, **262**, 737–746.
81 R. Chang, S. Kim, S. Lee, S. Choi, M. Kim and Y. Park, *Front. Energy Res.*, 2017, **5**, 17.
82 K. Song, W. Kim, S. Park, J.-H. Bang, C. W. Jeon and J.-W. Ahn, *Chem. Eng. J.*, 2016, **301**, 51–57.
83 K. Song, Y.-N. Jang, W. Kim, M. G. Lee, D. Shin, J.-H. Bang, C. W. Jeon and S. C. Chae, *Chem. Eng. J.*, 2012, **213**, 251–258.
84 Y. I. Svenskaya, H. Fattah, O. A. Inozemtseva, A. G. Ivanova, S. N. Shtykov, D. A. Gorin and B. V. Parakhonskiy, *Cryst. Growth Des.*, 2018, **18**, 331–337.
85 M. Abebe, N. Hedin and Z. Bacsik, *Cryst. Growth Des.*, 2015, **15**, 3609–3616.
86 A. E. Morandeau and C. E. White, *Chem. Mater.*, 2015, **27**, 6625–6634.
87 Z. Zhang, Y. Xie, X. Xu, H. Pan and R. Tang, *J. Cryst. Growth*, 2012, **343**, 62–67.
88 H. Tang, J. Yu and X. Zhao, *Mater. Res. Bull.*, 2009, **44**, 831–835.
89 H. Lu, B. Zhong, B. Liang and Y. Zhang, *J. Chem. Eng. Chin. Univ.*, 2002, **16**, 97–100.
90 Q. Chen, J. Wang, Z. Zhang, X. Wang, L. Yang, B. Zhong and X. Yang, *Chem. Ind. Eng. Prog.*, 2016, **35**, 3714–3719.
91 J. Zhao, X. Song, Y. Sun, B. Chen and J. Yu, *Cryst. Res. Technol.*, 2015, **50**, 277–283.
92 B. Njegić Džakula, J. Kontrec, M. Ukrainczyk, S. Sviben and D. Kralj, *Cryst. Res. Technol.*, 2014, **49**, 244–256.
93 M. D. Luque de Castro and F. Priego-Capote, *Ultrason. Sonochem.*, 2007, **14**, 717–724.
94 H. Cheng, X. Wang, B. Wang, J. Zhao, Y. Liu and F. Cheng, *J. Cryst. Growth*, 2017, **469**, 97–105.
95 Q. Chen, W. Ding, H. Sun, T. Peng and G. Ma, *Energy*, 2020, **206**, 118148.
96 W. Ding, Q. Chen, H. Sun and T. Peng, *J. $CO_2$ Util.*, 2019, **34**, 507–515.
97 Q. Chen, W. Ding, H. Sun, T. Peng and G. Ma, *ACS Sustain. Chem. Eng.*, 2020, **8**, 11649–11657.
98 B. Yang, M. Yang, B. Wang, X. Fang and Q. Wan, *Mater. Res. Express*, 2019, **6**, 045042.
99 Y. Gong, X. Zhu, Z. Yang, X. Zhang and C. Li, *RSC Adv.*, 2022, **12**, 26556–26564.
100 L. Ma, X. Niu, J. Hou, S. Zheng and W. Xu, *Thermochim. Acta*, 2011, **526**, 163–168.
101 Z. Miao, H. Yang, Y. Wu, H. Zhang and X. Zhang, *Ind. Eng. Chem. Res.*, 2012, **51**, 5419–5423.
102 M. de Beer, J. P. Maree, L. Liebenberg and F. J. Doucet, *Waste Manage.*, 2014, **34**, 2373–2381.
103 R. K. Tewo, J. P. Maree, S. Ruto, H. L. Rutto and L. K. Koech, *Chem. Eng. Commun.*, 2017, **204**, 1412–1419.
104 S. Liu, C. Yang, T. Zhang, W. Liu, F. Jiao and W. Qin, *Sep. Purif. Technol.*, 2023, **314**, 123537.
105 H. Tan, M. Ye, X. Su, X. Ma, F. Dong and F. Yang, *J. Therm. Anal. Calorim.*, 2022, **147**, 14115–14121.
106 F. Laasri, A. Carrillo Garcia, M. Latifi and J. Chaouki, *Waste Manage.*, 2023, **171**, 482–490.
107 Y. Yu and L. Li, *ISIJ Int.*, 2020, **60**, 2291–2300.
108 J. Zhao, H. Su, H. Zuo, J. Wang and Q. Xue, *J. Cleaner Prod.*, 2020, **267**, 122002.
109 N. Mihara, D. Kuchar, Y. Kojima and H. Matsuda, *J. Mater. Cycles Waste Manage.*, 2007, **9**, 21–26.
110 S. R. Motaung, J. N. Zvimba, J. P. Maree and A. V. Kolesnikov, *Water SA*, 2015, **41**, 369–374.
111 K. Uiga, E. Rikmann, I. Zekker and T. Tenno, *Proc. Est. Acad. Sci.*, 2020, **69**, 323–330.
112 S. J. Eng, R. J. Motekaitis and A. E. Martell, *Inorg. Chim. Acta*, 2000, **299**, 9–15.
113 K. Wang, S. Lin and Z. Z. Ran, *J. Therm. Anal. Calorim.*, 2023, **148**, 7357–7368.
114 S. Piché and F. Larachi, *Chem. Eng. Sci.*, 2006, **61**, 7673–7683.
115 P. Córdoba, R. Ochoa-Gonzalez, O. Font, M. Izquierdo, X. Querol, C. Leiva, M. A. López-Antón, M. Díaz-Somoano, M. Rosa Martinez-Tarazona, C. Fernandez and A. Tomás, *Fuel*, 2012, **92**, 145–157.
116 E. Álvarez-Ayuso, X. Querol and A. Tomás, *Chemosphere*, 2006, **65**, 2009–2017.
117 M. Zhu, B. H. Tian, S. Luo, Y. Z. Chi, D. Aishajiang, Y. Zhang and M. Yang, *Resour. Conserv. Recycl.*, 2022, **186**, 106556.
118 O. S. L. Bruinsma, D. J. Branken, T. N. Lemmer, L. van der Westhuizen and S. Rossouw, *Desalination*, 2021, **511**, 115096.
119 Kuldeep, W. D. Badenhorst, P. Kauranen, H. Pajari, R. Ruismäki, P. Mannela and L. Murtomäki, *Membranes*, 2021, **11**, 718.
120 X. Xia, L. Q. Zhang, X. L. Yuan, C. Y. Ma, Z. L. Song and X. Q. Zhao, *Environ. Eng. Sci.*, 2021, **38**, 886–898.
121 L. L. Guo, Z. Wu, H. Wang, H. L. Yan, F. S. Yang, G. X. Cheng and Z. X. Zhang, *Chem. Eng. J.*, 2023, **455**, 140689.
122 J. X. Xu and W. S. Lin, *Energy*, 2021, **227**, 120416.

123 H. Hu and M. B. Wu, *J. Mater. Chem. A*, 2020, **8**, 7066–7082.
124 L. Monat, S. Chaudhury and O. Nir, *ACS Sustain. Chem. Eng.*, 2020, **8**, 2490–2497.
125 N. V. Kovalev, T. V. Karpenko, N. V. Sheldeshov and V. I. Zabolotskii, *Membr. Membr. Technol.*, 2020, **2**, 391–398.
126 W. Gao, Q. Fang, H. Yan, X. Wei and K. Wu, *Membranes*, 2021, **11**, 152.